

Gas Segregation in Dykes and Sills

T. Menand and J. C. Phillips



Department of Earth Sciences, University of Bristol, Queen's Road, Bristol BS8 1RJ, UK., T.Menand@bristol.ac.uk, J.C.Phillips@bristol.ac.uk



Figure 1: Etna (Bocca Nuova) erupts dense ash clouds on 31 Oct 2002.

Basaltic volcanoes may persistently degas for years to millenia, erupting relatively little degassed lava and thus requiring efficient physical separation of volatiles from magma over very long periods of time. Mass balance requires that large amounts of magma must be processed during gas segregation, which would imply growth of the volcanic plumbing system by influx of new, gas-bearing magma stored at shallow depth where it degasses. Alternatively, long-lived degassing can be achieved by recirculation of magma between shallow parts of the plumbing system where over-saturated volatiles are extracted, and deeper parts of the system where degassed magma is recycled. Proposed degassing processes include bubble coalescence, convection processes in conduits, and foam development in reservoirs. However, as suggested by seismic studies at Kilauea Volcano (Hawaii) and geochemical studies at Mt. St. Helens, the plumbing system geometry and connectivity could provide an important control on magma movement in those systems and thus on gas segregation processes in basaltic magmas. We investigated 1) how the plumbing system geometry and connectivity affect the circulation of magma and 2) how this circulation impacts gas segregation. This investigation was undertaken to examine processes that might affect gas segregation from magmas in the vicinity of underground openings at the potential high-level radioactive waste repository at Yucca Mountain, Nevada.



Figure 2: How does the plumbing system affect gas segregation?

1. EXPERIMENTS

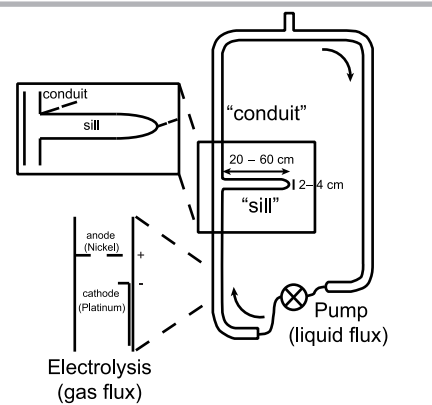


Figure 3: Gas segregation is investigated in the simple geometry of a vertical conduit connected to a horizontal intrusion by means of analogue experiments. Degassing is simulated by electrolysis, producing micrometric bubbles in viscous mixtures of water and golden syrup.

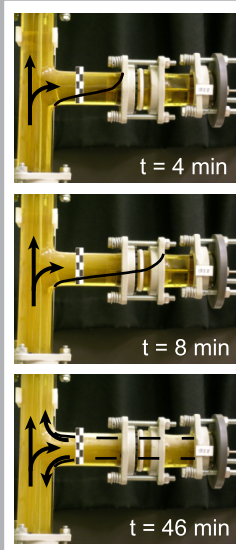


Figure 4: Bubbles induce a buoyancy-driven exchange flow between conduit and intrusion.

Bubbles rise and segregate in intrusion as foam at the top and degassed fluid layer at the bottom.

Steady-state influx of bubbly fluid from conduit into the intrusion is balanced by outward flux of lighter foam and denser degassed fluid.

2. STEADY-STATE GAS SEGREGATION

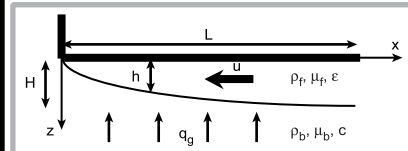


Figure 5: Gas segregates as a foam in intrusion.

Notations:

- ρ_l, ρ_b, ρ_f : density of pure liquid, bubbly fluid and foam,
- μ_l, μ_b, μ_f : viscosity of pure liquid, bubbly fluid and foam,
- d : average bubble diameter,
- c, ϵ : bubbly and foam gas fraction ($\epsilon = 0.7$ typically),
- g : gravitational acceleration,
- L : length of bubbly current,
- D : thickness of intrusion,
- h : local foam height,
- u : foam velocity,
- q_g : bubbly flux feeding the foam,
- x : horizontal position along the foam,
- z : vertical position along the foam,
- H : height of magmatic intrusion,
- T_b, T_f, T_s : bubble, foam and solidification time scales,
- κ : thermal diffusivity,
- λ : dimensionless thermal constant,
- Q_l : experimental fluid flux in vertical conduit,
- Q_g : experimental gas flux and gas return rate,
- Q_s, Q_{ex}, Q_D : supply rate of gas-rich magma, exchange rate of bubbly magma in the intrusion and degassed-magma return rate.

- Foam is modelled as a gravity current resisted by internal viscous stresses.
- Analysis is based on Jaupart & Vergnolle (1989).
- Foam boundary conditions: i) no slip on top, and ii) no shear stress at interface.
- Shape of the foam by steady-state mass balance:

$$h(x) = \left[\frac{cd^2L^2}{\epsilon(\epsilon-c)(1-\epsilon)^{5/2}} \right]^{1/4} \left[\frac{x(L-x)}{2L} \right]^{1/4}$$

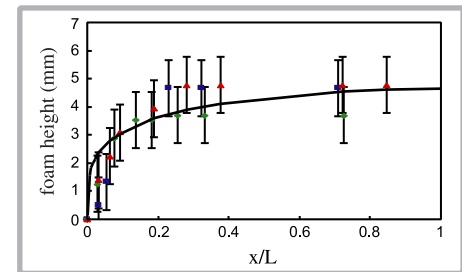


Figure 6: Steady-state foam height along tube. Each set of symbols represents an experiment. Experiments have identical gas flux Q_g but different fluid flux in vertical conduit: red triangles, $Q_l = 0$; green diamonds, $Q_l = 9Q_g$; blue squares, $Q_l = 79Q_g$. Solid line is model prediction with bubbly gas fraction $c = 0.06$ and foam gas fraction $\epsilon = 0.8$.

- Gas segregation processes and rates in an intrusion are independent of changes in fluid supply rate (Figure 6).
- Exchange of fluid and gas between a conduit and a horizontal intrusion is predominantly driven by gas segregation in the intrusion.

3. TIME SCALES & THERMAL VIABILITY

Time scales

- Bubble rise time in intrusion (from Stokes law): $T_b = \frac{12 \mu_l D}{\rho_l g d^2}$
- Foam formation time (from average foam height and velocity): $T_f = \frac{12 \mu_l L^{1/2}}{\rho_l g d^{3/2}} \epsilon^{3/4} [c^3(1-\epsilon)^{5/2}(\epsilon-c)]^{1/4}$
- Cooling and solidification time (by conduction): $T_s = \frac{D^2}{16\kappa\lambda^2}$

Gas segregation is thermally viable when $T_b, T_f < T_s$

Sill, $D = 10$ m [32.8 ft], $L = 1$ km [0.6 mi], $d = 1$ mm [0.4 in]

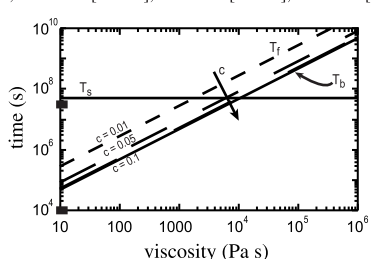


Figure 7: Gas segregation time scales for a sill as function of magma viscosity, bubbly gas fraction, average bubble diameter and sill dimension (magma density $\rho_l = 2700$ kg/m³). Thick black ticks on time axis represent 1 day and 1 year.

• Gas segregation by foam formation in sills is a thermally viable process for intermediate as well as basaltic magmas.

Gas segregation in dykes

• Horizontally propagating dykes are thinner and higher than sills. This implies larger bubble rise time scale T_b and smaller solidification time scale T_s (Figure 8).

• Thus, gas segregation is more efficient in sills than in horizontally propagating dykes.

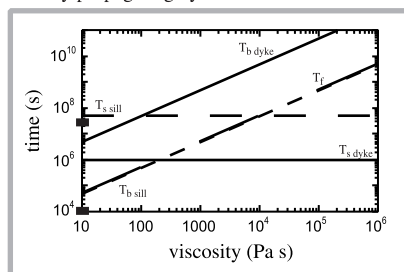
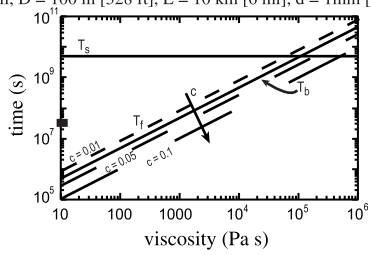
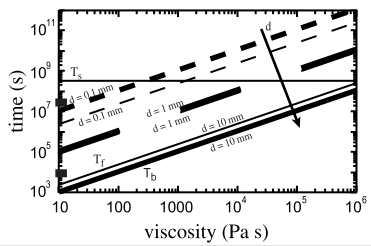


Figure 8: Gas segregation time scales for a dyke, 2 m [6.6 ft] thick and 1 km [0.6 mi] long and high, and a sill 10 m [32.8 ft] thick and 1 km long and wide (bubbly gas fraction $c = 0.1$, bubble diameter $d = 1$ mm [.04 in], magma density = 2700 kg/m³). Thick black ticks on time axis represent 1 day and 1 year.

Sill, $D = 100$ m [328 ft], $L = 10$ km [6 mi], $d = 1$ mm [0.4 in]



Sill, $D = 25$ m [82 ft], $L = 2.5$ km [1.6 mi], $c = 0.1$



4. ERUPTIVE IMPLICATIONS

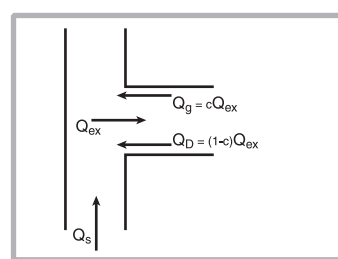


Figure 9: Gas segregation induces a steady-state exchange flow rate Q_{ex} of exsolved gas (foam) return flow Q_g and degassed-magma return flow Q_D , that is independent of magma supply rate Q_s : $Q_{ex} = Q_g + Q_D$.

- Steady-state gas return flux (foam):

$$Q_g = \frac{c \rho_l g d^2 L^2}{12 \mu_l \epsilon}$$
- Degassed-magma return flux (by mass balance):

$$Q_D = \frac{(1-c) \rho_l g d^2 L^2}{12 \mu_l \epsilon}$$
- Gas segregation exchange rate:

$$Q_{ex} = \frac{\rho_l g d^2 L^2}{12 \mu_l \epsilon}$$

- Strombolian activity when $Q_s < Q_{ex}$ and more explosive eruptions when $Q_s > Q_{ex}$.
- Transition between these two behaviours when both fluxes are comparable: $Q_s \sim Q_{ex}$.

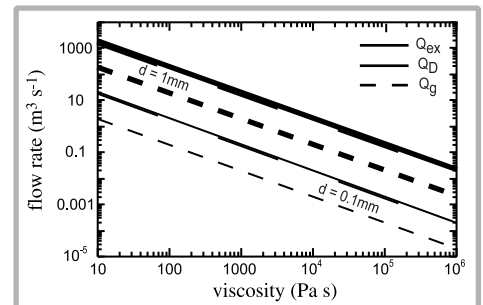


Figure 10: Exchange flow rate Q_{ex} , exsolved gas return rate Q_g and degassed magma return rate Q_D as function of magma viscosity and average bubble diameter. Intrusion is 2.5 km [1.6 mi] long and wide, 25 m [82 ft] thick. Bubbly gas fraction $c = 0.1$.

5. APPLICATION TO STROMBOLI VOLCANO

- These general physical principles can be applied to Stromboli volcano and are consistent with independent field data.
- Gas segregation at Stromboli is thought likely to occur in a shallow reservoir of sill-like geometry, 2.5 km [1.6 mi] long and wide and 25 m [82 ft] thick, at 3.5 km [2.2 mi] depth with exsolved gas bubbles 0.1–1 mm [.04–.04 in] in diameter.
- For this set of parameters, gas segregation occurs on a time scale shorter than the magma residence time.
- Transition between eruptions of gas-poor, high crystallinity magmas and violent explosions that erupt gas-rich, low crystallinity magmas are calculated to occur at a critical magma supply rate of order 0.1–1 m³ s⁻¹.

Reference

Jaupart, C., Vergnolle, S., 1989. The generation and collapse of a foam layer at the roof of a basaltic magma chamber. J. Fluid Mech. 203, 347–380.

Acknowledgements

This poster was prepared to document work performed by the Center for Nuclear Waste Regulatory Analyses (CNWRA) and its contractors for the Nuclear Regulatory Commission (NRC) under Contract No. NRC-02-02-012. The activities reported here were performed on behalf of the NRC Office of Nuclear Material Safety and Safeguards, Division of High Level Waste Repository Safety. This paper is an independent product of the CNWRA and does not necessarily reflect the view or regulatory position of the NRC.